Rayleigh–Taylor instability of violently collapsing bubbles

Hao Lin
University of California at Berkeley, Department of Mechanical Engineering, Berkeley, California 94720-1740

Brian D. Storey
Franklin W. Olin College of Engineering, Needham, Massachusetts 02492-1245

Andrew J. Szeri
University of California at Berkeley, Department of Mechanical Engineering, Berkeley, California 94720-1740

(Received 17 January 2001; accepted 9 May 2002; published 8 July 2002)

In a classical paper Plesset has determined conditions under which a bubble changing in volume maintains a spherical shape. The stability analysis was further developed by Prosperetti to include the effects of liquid viscosity on the evolving shape modes. In the present work the theory is further modified to include the changing density of the bubble contents. The latter is found to be important in violent collapses where the densities of the gas and vapor within a bubble may approach densities of the liquid outside. This exerts a stabilizing influence on the Rayleigh–Taylor mechanism of shape instability of spherical bubbles. A comparison with experimental data shows good agreement with the new theory; the Rayleigh–Taylor instability does provide an extinction threshold for violently collapsing bubbles. It is also explained why earlier works did not produce a slope in the Rayleigh–Taylor stability curve that conforms with that of the present work. © *2002 American Institute of Physics.* [DOI: 10.1063/1.1490138]

In a classical paper, Plesset[1] has analyzed the interface of a bubble undergoing a change in volume. He found that bubbles do not always retain their spherical symmetry. The theory was further developed by Prosperetti[2] who included the effects of liquid viscosity in what had been an inviscid analysis. Numerous researchers have investigated the stability of spherical bubbles in a variety of applications. Of greatest interest in the present work are those papers dealing with the especially violent collapses characteristic of sonoluminescence bubbles: Hilgenfeldt *et al.*,[3] Wu and Roberts,[4] Hao and Prosperetti[5] as well as experimental works by Holt and Gaitan,[6] and Ketterling and Apfel.[7]

The practical importance of the spherical stability of collapsing bubbles is manifest in two important ways. In applications such as sonochemistry, the intense energy focusing of the violent collapse is responsible for the high temperatures (and subsequent reactions) in the bubble interior. If the bubble collapse is not spherical, it is thought that the focusing of the energy is not as intense and the maximum achievable temperatures correspondingly lower; this would have an influence on the overall rate of chemical production. In multi-bubble sonoluminescence, light production is predicted to be diminished if the collapses are ellipsoidal.[8] In single bubble sonoluminescence, spherical instability is a critical phenomenon that participates in the delineation of the accessible experimental parameter space.[3]

Following the latter reference of Hilgenfeldt *et al.*, we consider two types of instabilities: parametric and Rayleigh–Taylor. The parametric instability evolves over several bubble oscillations. If a disturbance is found to grow over many cycles, it is assumed that the bubble will break up under these conditions, although such a conclusion is properly the domain of nonlinear analysis. In contrast, the Rayleigh–Taylor (RT) instability occurs during a single violent collapse of the bubble. The inward acceleration becomes so great that the bubble can become unstable, for the same reason that under gravity a layer of heavy fluid over a lighter one can be unstable.

In this paper we modify the classical equations of Plesset for the evolution of nonspherical disturbances to account for the changing density of the contents of the bubble. Previous efforts with similar goals include Ref. 9.

During a violent collapse, the density of the bubble contents can be quite high. As the density difference across the interface is the driver of RT instability, a higher gas density during the brief period of the most extreme interfacial acceleration provides a stabilizing effect.

We have recently developed[10] an approximation for inertially-driven spatial inhomogeneities in the bubble interior, consisting of a velocity profile linear in radius and a pressure field that is quadratic in radius. The approximation has been verified by careful comparisons with direct numerical simulations (DNS). The expression for the velocity potential ϕ is

$$\phi = \tfrac{1}{2}\,(\dot{R}/R)\,r^2, \tag{1}$$

where $R(t)$ is the bubble radius, r is the radial coordinate, and the over-dot denotes differentiation with respect to time. The expression for the pressure in the bubble interior is

$$p(r,t) = p_c(t) - \overline{\rho}(t)(\partial\phi/\partial t + \tfrac{1}{2}|\nabla\phi|^2), \tag{2}$$

where p_c is the pressure at bubble center and $\overline{\rho}$ is the (spatially uniform) density,

$$\overline{\rho}(t) \equiv \rho_0 (R/R_0)^{-3}. \tag{3}$$

Here, the subscript 0 denotes the ambient quantity. We have written the pressure field in the form suggestive of the Bernoulli equation, which we shall use shortly in the dynamical boundary condition on the interface. The assumption of a uniform density field (3) is of course naive, as the relatively cold wall during a violent collapse results in an increased gas density in the vicinity. The suitability of the uniform density field is discussed at some length in Ref. 10.

We shall follow the formulation of Plesset closely, with a slight modification at the outset to account for the changing gas density and inertially modified pressure. We suppose the spherical interface to be distorted from $R(t)$ to a new radial position $r_s = R(t) + a_n(t) Y_n(\theta, \phi)$, where $Y_n(\theta, \phi)$ is a spherical harmonic of degree n and $a_n(t)$ its corresponding time-dependent amplitude of the disturbance. The radial velocity of the disturbed bubble wall is then $u = \dot{R} + \dot{a}_n Y_n$. The velocity potentials for the base flow plus disturbance flow are

$$\begin{aligned} &\phi_g = \phi_g^0 + \phi_g' = -(\dot{R} r^2/2R) + b_g r^n Y_n, \quad r < r_s \ \text{(gas)}, \\ &\phi_l = \phi_l^0 + \phi_l' = (R^2 \dot{R}/r) + b_l r^{-(n+1)} Y_n, \quad r > r_s \ \text{(liquid)}, \end{aligned} \tag{4}$$

where the subscript g denotes gas and l denotes liquid. It is in the inclusion of the base flow [i.e., the first term of ϕ_g in (4)] where the present analysis first differs from prior theory, including Ref. 9. In Ref. 9, the authors simply take the gas density to be time dependent in the formulation of Plesset and later authors. This may be regarded as an estimate, as the theory of Plesset and later authors is in fact developed for a constant and uniform density. Nevertheless, the equations we derive below are similar to those obtained in Ref. 9.

Note that the disturbances in the velocity potential satisfy

$$\nabla^2 \phi_g' = 0, \tag{5}$$

which suggests an infinite speed for the propagation of associated pressure disturbances. Thus there is an implicit assumption that the time it takes for information to travel through the bubble is much smaller than the time scale for the instability, owing to the smallness of the bubble and the magnitude of the sound speed.

Now we turn to the conditions that must be satisfied at the interface. The radial velocities in both gas and liquid must match: $-(\partial \phi_g/\partial r)_{r_s} = -(\partial \phi_l/\partial r)_{r_s} = \dot{R} + \dot{a}_n Y_n$. This allows one to determine the unknown coefficients b_g and b_l, which leads to

$$\begin{aligned} \phi_g &= -\frac{\dot{R} r^2}{2R} + \frac{r^n}{n R^{n-1}} \left[\frac{\dot{R}}{R} a_n - \dot{a}_n \right] Y_n, \\ \phi_l &= \frac{R^2 \dot{R}}{r} + \frac{R^{n+2}}{(n+1) r^{n+1}} \left[\dot{a}_n + 2 a_n \frac{\dot{R}}{R} \right] Y_n. \end{aligned}$$

The second condition to be applied at the interface is the balance of normal stresses. The pressure at the interface in both liquid and gas can be obtained from the Bernoulli integral:

$$p_g = p_c(t) + \rho_g [(\partial \phi_g/\partial t) - \tfrac{1}{2} (\partial \phi_g/\partial r)^2]_{r_s}, \tag{6}$$

$$p_l = p_\infty(t) + \rho_l [(\partial \phi_l/\partial t) - \tfrac{1}{2} (\partial \phi_l/\partial r)^2]_{r_s}, \tag{7}$$

where p_∞ is the pressure at infinity, and we use $\overline{\rho}$ for ρ_g. In the absence of the perturbation (6) recovers (2). We evaluate these expressions to first order in a_n and match them at the interface $r = r_s$. This yields both a linearized form of the Rayleigh–Plesset equation (at zeroth order, not shown here) and a second order ODE governing $a_n(t)$ (at first order):

$$\begin{aligned} &\left(\frac{\rho_l}{n+1} + \frac{\rho_g}{n} \right) \ddot{a}_n + \frac{3\rho_l}{n+1} \frac{\dot{R}}{R} \dot{a}_n + \left[\left(\frac{\rho_g}{n} - \frac{\rho_l}{n+1} \right) \ddot{R} \right. \\ &\qquad \left. + \frac{n+2}{R^2} \sigma \right] (n-1) \frac{a_n}{R} = 0. \end{aligned}$$

As in the original work by Plesset, the preceding analysis does not take into account the effect of viscosity in the liquid. This plays a significant role in shape oscillation. Because Prosperetti's[2] viscous correction applies only to the liquid, we can follow his procedure and obtain a similar correction in the present case. In the interest of brevity, we just present the result without derivation. In order to compare the various approaches, we write Prosperetti's results [Eq. (7) of Ref. 5] in the following way:

$$\ddot{a}_n + \tilde{B}_n(t) \dot{a}_n - \tilde{A}_n(t) a_n = 0, \tag{8}$$

where the subscript n denotes the nth harmonic and the time-dependent coefficients are

$$\begin{aligned} \tilde{A}_n(t) &= (n-1) \left[\frac{\ddot{R}}{R} - (n+1)(n+2) \frac{\sigma}{\rho_l R^3} - 2 \frac{\nu \dot{R}}{R^3} \left((n+1) \right. \right. \\ &\qquad \left. \left. \times (n+2) - \frac{n(n+2)}{1 + 2\delta/R} \right) \right], \\ \tilde{B}_n(t) &= \frac{3\dot{R}}{R} + \frac{2\nu}{R^2} \left[-(n-1)(n+1)(n+2) + \frac{n(n+2)^2}{1 + 2\delta/R} \right]. \end{aligned}$$

In this equation the boundary layer thickness δ is defined through[3,4] $\delta = \min(\sqrt{\nu/\omega}, R/2n)$, and ω is the acoustic driving frequency. The influence of the gas density in the present model is then taken into account through the following alterations on $\tilde{A}_n$ and $\tilde{B}_n$:

$$\begin{aligned} A_n &= \frac{\rho_l/(n+1)}{\rho_g/n + \rho_l/(n+1)} \tilde{A}_n - \frac{\rho_g/n}{\rho_g/n + \rho_l/(n+1)} \\ &\qquad \times (n-1)(\ddot{R}/R), \\ B_n &= [\rho_l/(n+1)]/[\rho_g/n + \rho_l/(n+1)] \, \tilde{B}_n. \end{aligned}$$

Hence the new evolution equation we propose is

$$\ddot{a}_n + B_n(t) \dot{a}_n - A_n(t) a_n = 0. \tag{9}$$

Clearly when $\rho_g \to 0$ this recovers the model of Plesset and Prosperetti.

An alteration of instability criteria can be expected to be significant only in the case of the strongest collapses. Hence we focus in what follows on the parameter range of single bubble sonoluminescence (SBSL).

To demonstrate the influence of gas density on the spherical instability of the bubble we solve (9) numerically along with the Rayleigh–Plesset equation. We choose the

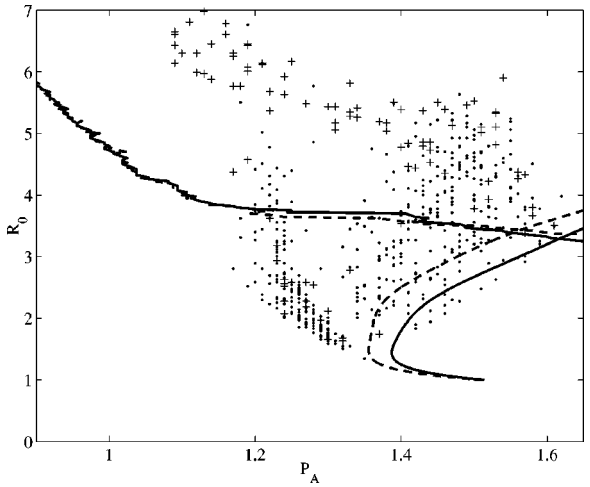

FIG. 1. The parametric and RT instability curves in the parameter space of single bubble sonoluminescence, computed both with (solid) and without (dashed) the effect of changing gas density developed in this paper. There is essentially no change to the parametric instability. The RT instability boundary is moved with the result that more violent collapses are now expected to be stable. The results are compared with experimental data for numerous experiments at various gas saturations provided by Ketterling (Ref. 7), with dots and plus signs denoting stable and unstable points, respectively.

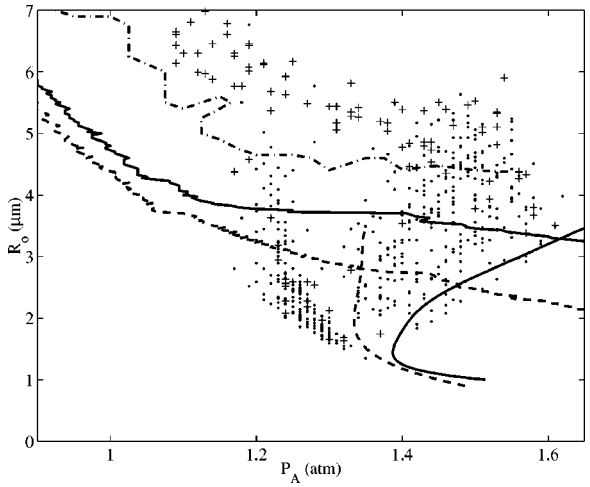

FIG. 2. Influence of the modeling of the spherical bubble dynamics on the determination of instability boundaries. Dashed curves are computed using a standard isothermal assumption (Ref. 3); solid curves utilize a reduced Rayleigh–Plesset model proposed by Storey and Szeri (Ref. 11); the dot–dashed curve is computed with radial dynamics from direct numerical simulation (Ref. 13). The experimental data is the same as in Fig. 1. The combination of the upper parametric curve (Ref. 12) and the solid RT curve constitutes an accurate prediction of the stability range in R_0-P_a space.

representative case of an argon bubble periodically driven at 32.8 kHz in liquid water at 293 K and an ambient pressure of 1 atm. The acoustic pressure amplitude, P_a, and bubble radius, R_0, are varied to observe the instability boundaries that limit the space where stable bubble oscillations can occur.

In Fig. 1 we show the instability boundaries in R_0-P_a space for both parametric and RT instabilities. We use a version of the Rayleigh–Plesset equation (RPE)[11] for radial dynamics $R(t)$. For all cases the stability criterion is developed for the $n=2$ mode, i.e., the most unstable mode. Following prior work by Hilgenfeldt *et al.*,[3] we add a random component with a Gaussian distribution and a standard deviation of 1 angstrom to simulate molecular fluctuations; also, following Ref. 3 we set the instability criterion to be $\max(|a_2(t)|/R(t))=1$, within one period of time, and when obtaining the RT instability boundary, average over many cycles at the same conditions to smooth out the randomness introduced to the formulation.

As one can observe from Fig. 1, the parametric instability is relatively unaffected by the changing gas density, with essentially no difference at low acoustic forcing. These trends are expected because this instability is a longer time scale phenomenon. The gas density is large only very briefly, and only during violent collapses. The Rayleigh–Taylor instability boundary is more strongly influenced by the changing gas density. The high gas density during the violent collapse exerts a stabilizing influence. The RT instability always occurs on the short time scale of the major collapse.

While the effect of gas density on the RT instability may seem modest in this diagram, it is worth emphasizing that the bubble dynamics are quite sensitive to the pressure amplitude. Hence, a small shift in the instability boundary means a big change in the bubble dynamics in the accessible region of parameter space. The effects of this modification also become evident when compared with experimental data in Fig. 1. The RT curve without changing gas density (dashed curve) is a little conservative, whereas the modified curve (solid) of the present theory better conforms to the boundary of stable bubbles found in the experiments.

There are two important observations to make about the results in Fig. 1. First, neither the old nor the new parametric stability curves constitute an accurate prediction when compared with experiments. Second, we thank a referee for pointing out that the RT curves we compute (with or without changing gas density), have positive slopes. In this respect the present results are very different from the findings in Refs. 3 and 9. We now consider the two points in turn.

In Ref. 12 it was shown that the choice of different equations for the spherical bubble dynamics has a strong influence on the parametric stability boundaries. This is again demonstrated in Fig. 2. The dashed parametric stability boundary is calculated using an isothermal approximation in the RPE.[3] It is clear that the stability boundary is far too conservative. The reason for this is clear: the insufficient damping in the isothermal model of radial dynamics leads to more vigorous afterbounces, which reduces the stability range. As a comparison, to compute the solid parametric stability curve of Fig. 2 (the same as in Fig. 1), we utilized a RPE proposed by Storey and Szeri,[11] which takes into account heat and mass transfer, non-equilibrium phase change, and chemical reactions. The improved heat transfer model makes the stability curve less conservative, because heat transfer acts to damp the radial oscillations that drive the long term growth of shape modes. Finally, the least conservative (dot–dashed) parametric stability curve uses $R(t)$ information computed from DNS of the compressible Navier–Stokes equations in the bubble interior,[13] as opposed to a RPE approach. The differences that result from these three models are evident in Fig. 2; the best prediction in the radial

dynamics (from DNS) results in the best prediction of the parametric stability boundaries.

Now we consider the second point, which concerns the slope of the RT curve in Fig. 1. In Fig. 2, we have added an RT stability curve on the left (dashed) with a vertical slope that is computed using the isothermal model following.[3] The (solid) RT curve in Fig. 2 (and in Fig. 1) is computed using the RPE model of Ref. 11. In computing both curves, we have included the effects of changing gas density. The source of this difference can be understood as follows. If the equations are made dimensionless, it becomes clear that the radial response of the bubble depends on a dimensionless driving pressure amplitude (Euler number), a dimensionless quantity related to the mass of gas in the bubble (which includes R_0), and dimensionless parameters associated with viscosity (Reynolds number) and surface tension (Weber number). For the bubbles of interest, the dependence of the gross features of the bubble dynamics on Reynolds and Weber numbers is weak. Now, the far field gas concentration in mass exchange equilibrium is a functional of $R(t)$; hence it is a function of P_a and R_0, with a weaker dependence on the Reynolds and Weber numbers. Similarly, the RT stability criterion is primarily a function of P_a and R_0, with weaker dependence on the Reynolds and Weber numbers. Hence, the RT stability criterion can be expected to follow roughly a curve of constant far field saturation. In previous works,[3,9] the RT criterion appears to overlay a level set of far field gas concentration that is somewhat higher than in the present work. Hence, the slope of the curve is negative in $P_a - R_0$ space. The present (solid) RT instability curve in Figs. 1 and 2 has a positive slope, following roughly a contour of lower far field gas concentration of about 0.05%. We find that for $P_a \geqslant 1.4$, larger bubbles are *stabilized*—with respect to RT—compared to smaller bubbles. This may seem counterintuitive. However, this is reasonable as it is well known that smaller bubbles collapse harder (with larger $R_{\max}/R_0$) in the sonoluminescence regime,[14] all other things being equal. The difference between the models is that in the previous works[3,9] the equation for radial dynamics contains approximations that lead to less internal pressure to resist the collapse than the model of Ref. 11, which was carefully verified against DNS. Evidently this determines how $R(t)$ [and especially $\ddot{R}(t)$] depends on P_a and R_0, and hence on which level set of far field gas concentration the RT stability curve (approximately) lies.

We remark that we are not the first authors to note that improved physical models have a rather dramatic effect on the RT instability. Although they do not report a RT stability curve, Prosperetti and Hao[15] show that the explosive growth in the maximum of a_2 over a cycle in the model of Ref. 3 (at $P_a = 1.3$ as R_0 varies between 3 and 4 μm) is absent with a more physically realistic model. Hao and Prosperetti[5] also note that better RP models improve the theoretical predictions for parametric instability.

In this paper we have developed a modification of the classical shape stability analysis of Plesset to account for the changing density of the bubble contents. The influence of gas density allows for more violent collapses to remain stable to shape disturbances.

In making quantitative predictions, we find that using a Rayleigh–Plesset model based on isothermal assumptions (a common assumption in the technical literature) results in overly conservative predictions of the accessible region of parameter space compared with experiments; but we emphasize that the basic interpretation of Hilgenfeldt *et al.* for the phenomena that determine when stable SBSL occurs is essentially correct. When the best efforts are made at accurately modeling both the radial and shape oscillations (including the correction for gas density), one finds excellent agreement with experimental data that falls well within the range of experimental uncertainty.

ACKNOWLEDGMENTS

Support for this work was provided, in part, by the National Science Foundation Program in Theoretical Physics, and by the Lawrence Livermore National Laboratory. The authors thank J. A. Ketterling for providing experimental data. A.J.S. would like to thank the Alexander von Humboldt Foundation for support and Professor W. Lauterborn for hosting a pleasant stay in Göttingen.

[1] M. S. Plesset, "On the stability of fluid flows with spherical symmetry," J. Appl. Phys. **25**, 96 (1954).
[2] A. Prosperetti, "Viscous effects on perturbed spherical flows," Quart. Appl. Math. **34**, 339 (1977).
[3] S. Hilgenfeldt, D. Lohse, and M. P. Brenner, "Phase diagrams for sonoluminescing bubbles," Phys. Fluids **8**, 2808 (1996).
[4] C. C. Wu and P. H. Roberts, "Bubble shape instability and sonoluminescence," Phys. Lett. A **250**, 131 (1998).
[5] Y. Hao and A. Prosperetti, "The effect of viscosity on the spherical stability of oscillating gas bubbles," Phys. Fluids **11**, 1309 (1999).
[6] R. G. Holt and D. F. Gaitan, "Observation of stability boundaries in the parameter space of single bubble sonoluminescence," Phys. Rev. Lett. **77**, 3791 (1996); "Experimental observations of bubble response and light intensity near the threshold for single bubble sonoluminescence in an air–water system," Phys. Rev. E **59**, 5495 (1999).
[7] J. A. Ketterling and R. E. Apfel, "Shape and extinction thresholds in sonoluminescence parameter space," J. Acoust. Soc. Am. **107**, L13 (2000); "Extensive experimental mapping of sonoluminescence parameter space," Phys. Rev. E **61**, 3832 (2000).
[8] B. Metten and W. Lauterborn, "Molecular dynamics approach to single-bubble sonoluminescence," in Nonlinear Acoustics at the Turn of the Millennium, Proceedings of the 15th International Symposium on Nonlinear Acoustics, Göttingen, Germany, 1–4 September 1999, edited by W. Lauterborn and T. Kurz; also see B. Metten, Ph.D. dissertation, University of Göttingen, 2000.
[9] U. H. Augsdörfer, A. K. Evans, and D. P. Oxley, "Thermal noise and the stability of single sonoluminescing bubbles," Phys. Rev. E **61**, 5278 (2000).
[10] H. Lin, B. D. Storey, and A. J. Szeri, "Inertially driven inhomogeneities in violently collapsing bubbles: The validity of the Rayleigh–Plesset equation," J. Fluid Mech. **452**, 145 (2002).
[11] B. D. Storey and A. J. Szeri, "A reduced model of cavitation physics for use in sonochemistry," Proc. R. Soc. London, Ser. A **457**, 1685 (2001).
[12] B. D. Storey, "Shape stability of sonoluminescence bubbles: A comparison of theory to experiments," Phys. Rev. E **64**, 017301 (2001).
[13] B. D. Storey and A. J. Szeri, "Water vapour, sonoluminescence and sonochemistry," Proc. R. Soc. London, Ser. A **456**, 1685 (2000).
[14] D. F. Gaitan and R. G. Holt, "Experimental observations of bubble response and light intensity near the threshold for single bubble sonoluminescence in an air–water system," Phys. Rev. E **59**, 5495 (1999).
[15] A. Prosperetti and Y. Hao, "Modeling of spherical gas bubble oscillations and sonoluminescence," Philos. Trans. R. Soc. London, Ser. A **357**, 203 (1999).